

A new method for producing highly concentrated non-aqueous dispersions of silver nanoparticles and the evaluation of their bactericidal activity

Roselaine da S. Oliveira · Marcos A. Bizeto ·
Ana M. A. Liberatore · Ivan H. J. Koh ·
Fernanda F. Camilo

Received: 9 May 2014 / Accepted: 28 October 2014 / Published online: 7 November 2014
© Springer Science+Business Media Dordrecht 2014

Abstract Different preparation methods of silver nanoparticles (AgNP) are well described in the literature, most of them in aqueous medium. Aqueous dispersions of AgNP normally have a limited capacity to tolerate high nanosilver concentrations. However, AgNP production in non-aqueous medium is still scarce although its exploitation for example, as coating for hydrophobic surfaces, would be of a huge importance in many technological applications. In this work, we report the chemical preparation of highly concentrated non-aqueous AgNP dispersions obtained by reduction of silver cation, from two distinct salt sources (AgNO_3 and AgBF_4), by 1-butanol in the presence of a biocompatible poly(ether-block-amide) copolymer, named PEBA. The highest concentration reached was around 5 mM, when it used AgBF_4 as silver source and 4 % (w/w) of a PEBA solution in

1-butanol. This AgNP concentration is notably higher than the values reported in aqueous medium. The AgNP formation was attested by UV–Vis spectroscopic analysis, which showed the characteristic strong plasmon band at 420 nm. The X-ray diffraction patterns confirmed the formation of a crystalline fcc silver metallic phase with particle diameters ranging from 5 to 10 nm accordingly to transmission electron microscopy examination. It was also observed that the AgNP dimensions are dependent on the PEBA and silver salt concentrations. The AgNP dispersions presented a very high antimicrobial activity against *E. coli* and *S. aureus* microorganisms, even in low concentration, attested by the Kirby-Bauer method.

Keywords Silver nanoparticle · Chemical reduction · Antimicrobial · Hydrophobic coating dispersion · Biocompatible polymer

Electronic supplementary material The online version of this article (doi:10.1007/s11051-014-2723-5) contains supplementary material, which is available to authorized users.

R. da S. Oliveira · M. A. Bizeto · F. F. Camilo (✉)
Laboratório de Materiais Híbridos, Instituto de Ciências Ambientais, Químicas e Farmacêuticas, Universidade Federal de São Paulo, Rua São Nicolau, 210, Diadema, São Paulo, SP CEP: 09913-030, Brazil
e-mail: ffcamilo@unifesp.br

A. M. A. Liberatore · I. H. J. Koh
Laboratório de Transplante Experimental de Órgãos, Departamento de Cirurgia, Universidade Federal de São Paulo, São Paulo, SP, Brazil

Introduction

Metallic nanomaterials (Ag, Au, Pt, Pd, etc.) have been extensively studied due to their interesting fundamental properties and many technological applications in fields such as nanoelectronics, nanophotonics, nanomedicine, chemical sensors, catalysts, and others (Pradeep 2009; Jain et al. 2008; Roduner 2006; Ray 2010). Among the family of transition metals, silver is one of particular interests thanks to its lower cost when compared to Au, Pd, and Pt and to its well-

established applications in the environmental and medical fields (Sharma et al. 2009; Sondi and Salopek-Sondi 2004; Chen and Schluesener 2008).

Two main synthetic approaches, the *bottom-up* and the *top-down* (Rao et al. 2005), are used to produce metallic nanoparticles. Silver nanoparticles (AgNP) can be produced by both (Poole and Owens 2003; Rotello 2004; Alonso et al. 2009; Tolaymat et al. 2010), but the *bottom-up* is the most used. It normally involves the chemical reduction of silver cations in aqueous solution containing a stabilizing agent to avoid the agglomeration of the AgNP (Ferrando et al. 2008; Cumberland and Lead 2009; Hu and Easterly 2009; Khaydarov et al. 2008). This synthetic method stands out for its simplicity, low cost, and possibility of large-scale preparation. The effectiveness of the chemical reduction route is very dependent on the appropriate choice of the silver salt precursor, stabilizing and reducing agents but also by experimental conditions such as reactants molar ratio, reaction time, pH, and temperature. These synthetic parameters strongly affect the nanoparticles size, shape, and stability and, consequently, their properties and potential applications (Krutyakov et al. 2008; Tolaymat et al. 2010).

Silver nitrate is the most common silver source for aqueous medium synthesis because of its lower cost and greater stability than other silver salts (Lee and Meisel 1982). Sulfate, perchlorate, and citrate salts are also utilized less frequently (Krutyakov et al. 2008; Tolaymat et al. 2010). It is noteworthy that these silver salts have limited solubility in organic solvents, thus this is an important obstacle to be transposed in order to achieve good results in non-aqueous medium synthesis of AgNP. One approach adopted to overcome this solubility restriction is the use of less common silver precursors (Tan et al. 2003), which implies in concerns related to the cost and reactant availability when considering large-scale preparation.

Regarding to the reducing agents employed in the aqueous medium AgNP syntheses, it is observed that NaBH_4 is the most used one, since it promotes the formation of very small and monodisperse nanoparticles, but this salt might also present solubility restrictions, as the common silver salts, in organic medium. In addition, it has the disadvantage of being toxic to human cells, even in small quantities, which becomes a concern when considering the use of AgNP dispersions in medical applications (Wang et al. 2008;

Chen et al. 2007). Aiming the use of this dispersion in the medical field, where even trace amounts of toxic residues are not acceptable, the use of a less toxic reducing agent is mandatory. These can be achieved by using citrate (Tan et al. 2003; Sileikaite et al. 2009; Pillai and Kamat 2004; Lee and Meisel 1982; Wang et al. 2008), ascorbic acid (Suber et al. 2005; Suber and Plunkett 2010; Lee et al. 2004; Yang et al. 2005; Sondi et al. 2003; Chen et al. 2007), and hydrazine (Yang et al. 2005; Zielińska et al. 2009; Nickel et al. 2000; Maillard et al. 2003). Although they are milder than sodium borohydride, they can, under appropriate experimental conditions, allow the production of AgNP in aqueous medium with desirable size and shape, without the formation of toxic residues.

It is known that nanoparticles dispersions are thermodynamically unstable and tend to agglomerate unless stabilizing agents are used during the synthesis to prevent agglomeration and/or excessive growth of the nanoparticles. In the aqueous medium synthesis, sodium dodecyl sulfate (Rodríguez-Gattorno et al. 2002; Patakfalvi et al. 2008; Tolaymat et al. 2010; Wang et al. 2008; Ghosh and Kolay 2008), polyvinylpyrrolidone (Zielińska et al. 2009; Patakfalvi et al. 2004; Tolaymat et al. 2010; Sun et al. 2002; Wang et al. 2005; Kim 2007), and polyvinyl alcohol (Zielińska et al. 2009; Patakfalvi et al. 2004; Tolaymat et al. 2010; Khanna et al. 2005) are the most used stabilizing agents (Yakovlev and Golubeva 2013).

Another issue that is common to the majority of AgNP aqueous dispersion is the low nanoparticles concentration (Solomon et al. 2007), typically varying from 1 to 50 mg l^{-1} (9.3×10^{-3} –0.47 mM) and the incompatibility with hydrophobic surfaces based on PTFE, silicone, PVC, PE, which are normally encountered in many medical devices. This fact hinders the use of AgNP as bactericidal coating, which is an important application for this nanomaterial.

Herein, we present a simple synthetic procedure in organic medium that overcomes the solubility restrictions of inorganic salts, presence of the toxic residue, and low concentration of AgNP as discussed before. We prepare highly concentrated hydrophobic dispersions of AgNP, using 1-butanol as both solvent and reduction agent. Two silver salts, AgNO_3 and AgBF_4 , were evaluated as precursors for nanoparticle formation and a poly(ether-block-amide) copolymer, called PEBA 2533 (Kontukhova et al. 2002) (Fig. 1), was used as stabilizing agent. This biocompatible

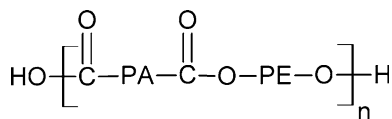


Fig. 1 PEBA 2533 structure composed by 80 % of a polyether (PE = poly(tetramethylene oxide)) and 20 % of a polyamide (PA = polyamide 12)

copolymer has excellent mechanical properties and solubility in 1-butanol. The antimicrobial activity of the dispersions was evaluated against *E. coli* and *S. aureus* microorganisms.

Experimental procedures

Materials and glassware cleaning

AgNO₃, AgBF₄, and 1-butanol were purchased from Sigma-Aldrich and used as received without purification. PEBA 2533 was obtained from Arkema Group. To avoid nanoparticles attachment and agglomeration to the glassware and storage vials, they were cleaned with piranha solution, extensively rinsed with milli-Q water and dried previously to the use.

AgNP preparation

First, PEBA 2533 was dissolved in 1-butanol in concentrations of 2, 3, or 4 % (w/w) with vigorous stirring under reflux. Solutions with concentration above 4 % of PEBA were not used due to the limited solubility of the polymer in 1-butanol. To a 10 ml sample of each PEBA solution, it added different

amounts of the silver salt (AgNO₃ or AgBF₄) and the mixture was refluxed for different times in order to promote the salt solubilization and Ag⁺ reduction. To remove the unreacted silver salt from the alcohol medium, the dispersions were treated as follows: first, 10 ml of deionized water was added to the AgNP dispersion with vigorous shaking, followed by letting the vial to rest to promote phase separation. To the aqueous phase, it was added a 0.1 M NaCl solution in order to promote the AgCl precipitation and to enable the quantification of the unreacted silver salt by gravimetric analysis. A schematic illustration of the procedure is presented in Fig. 1S of the supplementary information.

The phase containing AgNP was characterized and submitted to the microbiological assays. These samples are denoted in the text as PEBA_x%_ymM_AgA_zmin, where *x* is the PEBA concentration (w/w in %), *y* is the AgA initial concentration (in mM), *A* is the anion of the silver salt, and *z* is the reflux time in minutes. The concentration of silver nanoparticles in the dispersions was determined by the difference between the initial and remaining amount of Ag⁺. The samples abbreviations prepared in this work and their composition are listed in Table 1.

Equipment descriptions

X-ray diffraction patterns (XRDP) of the films were recorded on a Rigaku diffractometer model Miniflex using Cu-K_α radiation. Thermogravimetric analyses (TGA) were performed in a Shimadzu thermoanalyser TA-60, under synthetic air atmosphere with a flux of 100 cm³ min⁻¹ and a heating rate of 10 °C min⁻¹.

Table 1 Samples abbreviations and their descriptions

Sample abbreviation	Ag salt	Initial concentration of the silver salt (mM)	PEBA concentration (w/w) (%)	Reflux time (min)
PEBA 2 %_14.7 mM_AgNO ₃ _30 min	AgNO ₃	14.7	2	30
PEBA 3 %_14.7 mM_AgNO ₃ _30 min	AgNO ₃	14.7	3	30
PEBA 4 %_14.7 mM_AgNO ₃ _30 min	AgNO ₃	14.7	4	30
PEBA 4 %_14.7 mM_AgNO ₃ _10 min	AgNO ₃	14.7	4	10
PEBA 4 %_14.7 mM_AgNO ₃ _20 min	AgNO ₃	14.7	4	20
PEBA 4 %_14.7 mM_AgNO ₃ _40 min	AgNO ₃	14.7	4	40
PEBA 4 %_14.7 mM_AgBF ₄ _1 min	AgBF ₄	14.7	4	1
PEBA 4 %_14.7 mM_AgBF ₄ _3 min	AgBF ₄	14.7	4	3
PEBA 4 %_14.7 mM_AgBF ₄ _5 min	AgBF ₄	14.7	4	5

Fourier transformed infrared spectra (FTIR) were recorded on a Bomem spectrophotometer, model MB-102 using the DRIFT accessory with solid samples diluted in KBr. UV–Visible electronic absorption spectra (UV–Vis) of the dispersions were recorded on a Shimadzu spectrophotometer, model MultiSpec-1501 using quartz cuvettes. Zeta potential (ζ) and particle size distribution by dynamic light scattering (DLS) of the AgNP dispersions were measured on a Malvern Zetasizer nano ZS equipment. Transmission electron microscopy (TEM) images were recorded on a JEOL microscope model JEM 2100 operating at 200 kV. Samples were prepared by diluting the dispersion in isopropanol with the aid of an ultrasonic bath followed by deposition onto a carbon-coated Cu microgrid.

Microbiological assays

Staphylococcus aureus (ATCC 29213) and *Escherichia coli* (ATCC 25922) were grown in nutrient broth media (Difco) and incubated at 37 °C for 18–24 h. The culture was adjusted to 10^8 colony forming units (CFU)/ml by visual comparison to a 0.5 McFarland standard in sterile saline solution and spread over the plates containing Mueller–Hinton agar (Difco) using a sterile cotton swab in order to get a uniform microbial growth. Sterile filter papers disks with 6-mm diameter impregnated with 10 μ l of AgNP dispersions were placed on plates and incubated at 37 °C for 18–24 h. Experiments were carried out in duplicate.

Results and discussion

The AgNP dispersions were prepared from the chemical reduction of Ag^+ by 1-butanol affording Ag^0 and 1-butanal. The standard reduction potential (E^0) of Ag^+ to Ag^0 is +0.80 V. Since the standard oxidation potential of 1-butanol to 1-butanal is not available, we used the E^0 of the couple ethanol/ethanal (−0.20 V) to estimate the standard potential of the reaction (Lide 2004). The E^0 for the global reaction is positive ($E^0 = +1.00$ V), which indicates that the process is spontaneous. The formation of butanoic acid was discarded, due to the absence of water in the reaction medium (Habibi and Dadashpour 2013).

Despite its spontaneous character, this reaction does not proceed at a reasonable rate at room

temperature, so heating is necessary. The presence of PEBA 2533 is also of fundamental importance, otherwise, although the reaction occurs, the AgNP dispersion is not stable. In the absence of this copolymer, it observed nanoparticles agglomeration and adhering to the surface of the vial. It is worth to mention that these dispersions are hydrophobic, so in the presence of water two phases are produced, as it can be seen in the image presented in Fig. 2S of supplementary information. In this two-phase system, AgNP migrate to the alcoholic phase. In order to determine the best experimental conditions, the effect of reaction time, initial amount of silver salt, type of the silver salt, and percentage of PEBA 2533 in 1-butanol were evaluated as follows.

Influence of PEBA concentration

As commented before, PEBA has a crucial influence on the stability of the AgNP. Three different experiments containing 14.7 mM of AgNO_3 and 2, 3, or 4 % (w/w) of the PEBA dissolved in 1-butanol were refluxed during 30 min. The UV–Vis spectra of these samples registered immediately after the preparation are shown in Fig. 2. It is possible to observe a band centered at around 420 nm that corresponds to the typical surface Plasmon resonance of AgNP (Hunter and Fendler 2004; Yang et al. 2001). The dispersions produced with 2 and 3 % of PEBA precipitate after 2 and 4 months, respectively. This event was not observed in the dispersion prepared with 4 % of PEBA, which remained stable for at least one year.

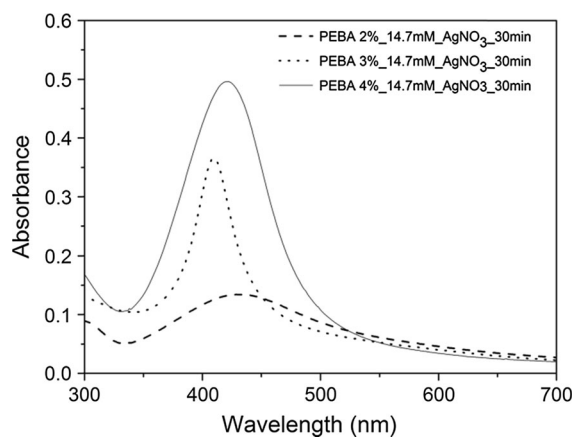


Fig. 2 UV–Vis electronic absorption spectra of the dispersions containing 14.7 mM of AgNO_3 in 2, 3, and 4 % of PEBA in 1-butanol after 30 min of reflux

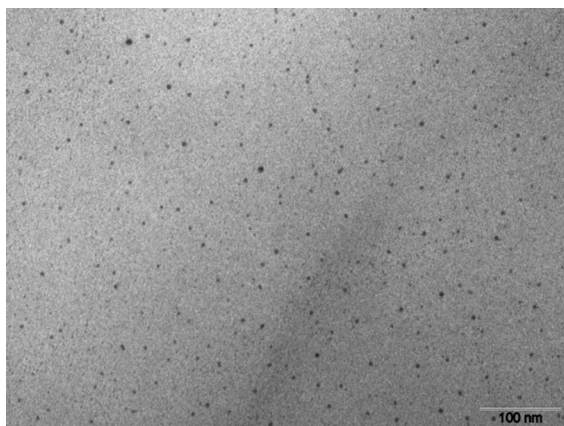


Fig. 3 TEM image of the PEBA 4 %_14.7mM_AgNO₃_30 min sample

The band profiles observed in Fig. 2 are not the same, suggesting that the resultant particle size and shape are different in each preparation. Intense plasmon bands are normally related to small nanoparticles, so it is possible to infer that the use of 4 % PEBA solution promoted the formation of smaller particles than those obtained in 2 and 3 % PEBA solutions, which is coherent with the stability differences.

In the TEM image of the sample PEBA 4 %_14.7mM_AgNO₃_30 min (Fig. 3), the AgNP appear as dark dots and the copolymer as bright areas. The TEM image (not shown here) of the sample containing 2 % of PEBA presents large particles and some agglomerates when compared to the samples containing 3 and 4 % of PEBA, fact that explains its low stability. Samples containing 3 and 4 % of PEBA show nanoparticles with spherical shape, similar size, and homogeneous distribution in the polymeric matrix, evidencing that the amount of PEBA is critical to maintain the long-term stability of the AgNP dispersion in 1-butanol. Due to this finding, all further studies to achieve the best experimental conditions were performed with the 4 % PEBA solution.

The measured Zeta potentials of these alcoholic AgNP dispersions were close to zero. Considering the particle surface charge, this would imply in an unstable dispersion with tendency for nanoparticle agglomeration. However, since these dispersions remain stable for at least one year, we can assume that the copolymer is acting as a dispersing agent for the nanoparticles and it is the responsible for the dispersion stability.

Another evidence of the stabilization character of the PEBA is given by the size of particles in the dispersion determined by DLS (Fig. 3S of supplementary information). The PEBA 4 %_14.7mM_AgNO₃_30 min sample presents a dynamic diameter of 2,492 nm with a low polydispersity index (PDI). Since this diameter is much bigger than the size of the AgNP observed in TEM image (Fig. 3) and it is also bigger than the particles of pure PEBA dispersion, it is reasonable to assume that PEBA is acting as dispersing agent for the nanoparticles.

Influence of reaction time

To determine the time required for the maximum Ag⁺ conversion in Ag⁰ using the 4 % PEBA 1-butanol solution, four experiments were performed using a fixed concentration of 14.7 mM of AgNO₃ and varying the reflux time (10, 20, 30, or 40 min). All the dispersions became yellow during the course of the reaction. Precipitation started to be observed after 50 min of reaction. The UV–Vis spectra of these dispersions are shown in Fig. 4, where it is possible to observe the characteristic Plasmon band of AgNP at 420 nm (Hunter and Fendler 2004; Yang et al. 2001). In all registered spectra, the band profiles are similar, indicating that the reaction time may not influence the nanoparticles size and shape. The difference in the intensity of Plasmon band is attributed to the concentration of the AgNP in the dispersion. The maximum absorbance is achieved after 30 min. The AgNP

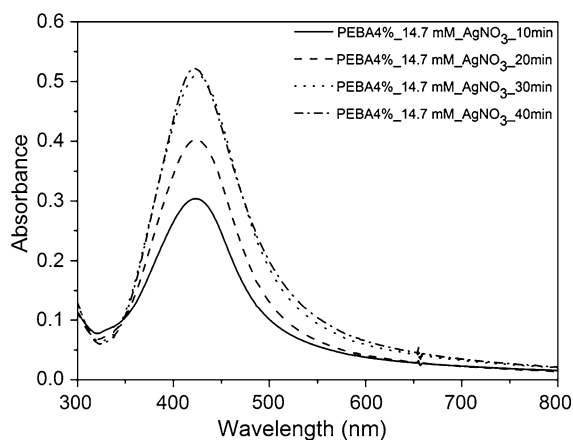


Fig. 4 UV–Vis electronic absorption spectra of the dispersions produced using 14.7 mM of AgNO₃ in 4 % PEBA 1-butanol solution at different reflux time intervals

concentrations, determined according to item 2.2, are around 0.6, 0.8, 1.0, and 1.0 mmol l^{-1} in the dispersions obtained after 10, 20, 30, and 40 min, respectively. Considering that the concentration of AgNP in aqueous medium is typically around 9.3×10^{-3} –0.47 mM, it is possible to affirm that these dispersions contain much higher AgNP concentration than the ones produced in aqueous solution.

Influence of silver salt

Due to the limited solubility of AgNO_3 in 1-butanol, AgBF_4 was also used as Ag^+ source in order to produce more concentrated AgNP dispersions. AgBF_4 is much more soluble in 1-butanol than AgNO_3 , even at room temperature, as can be seen in Fig. 4S of the supplementary information. Using the most promising experimental conditions found for the dispersions produced with AgNO_3 (4 % of PEBA in 1-butanol and 30 min of reflux time), one experiment using AgBF_4 was tested. Differently from what was observed in the procedure using AgNO_3 , the precipitation of AgNP started to be observed visually after 7 min of reflux. Thus, three experiments completed after 1, 3, and 5 min of reaction times were performed, and their UV–Vis spectra are shown in Fig. 5. It was not observed any Plasmon band intensity increasing after 3 min of reaction, as it can be seen in Fig. 5. Thus, it was assumed that 3 min is enough to produce the maximum concentration of AgNP when using AgBF_4 as silver source.

Due to the improved solubility of AgBF_4 in 1-butanol, experiments with more concentrated

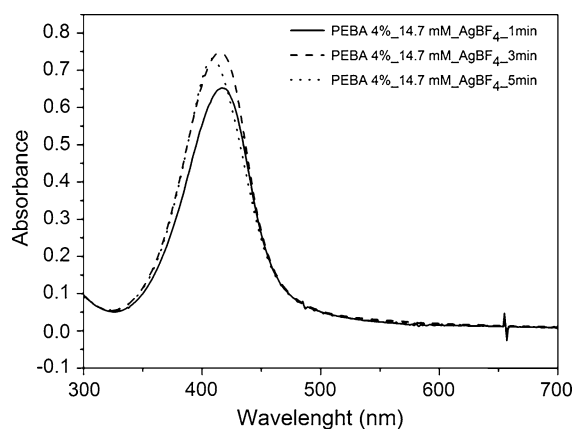


Fig. 5 UV-Vis electronic absorption spectra of the dispersions produced using 14.7 mM of AgBF_4 in 4 % of 1-butanol PEBA solution at different reflux time intervals

AgBF_4 solutions were also carried out. Procedures starting with 258, 152, 51.5, and 25.7 mM of AgBF_4 resulted in deep yellow dispersions, but not as stable as the one prepared with 14.7 mM of AgBF_4 , which remained without precipitation for at least one year.

The Zeta potentials determined for the dispersions produced with 14.7 mM of AgBF_4 in different reaction times were also close to zero, indicating that their nanoparticles are not charged and their stability is maintained by the dissolved PEBA, as previously discussed.

The AgNP concentration in the sample PEBA4 %_14.7 mM_ AgBF_4 _3 min, determined according to the item 2.2, is around 5 mmol l^{-1} , which is five times greater than the one prepared with AgNO_3 . TEM images of this sample (Fig. 6) indicate that the agglomeration of nanoparticles practically does not exist. The high AgNP concentration is clearly evidenced in this image, where it is also possible to observe spherical nanoparticles with diameters ranging from 5 to 10 nm.

Taking into account that samples PEBA4 %_14.7 mM_ AgBF_4 _3 min and PEBA4 %_14.7 mM_ AgNO_3 _30 min are the most concentrated achieved in this work, they were further characterized by FTIR, XRD, and TGA. For these analyses, 1-butanol was removed under reduced pressure at 60°C , resulting in self-supported yellow films. These films have hydrophobic properties similar to PEBA 2533 films (Djebbar et al. 1998). The films obtained for the samples PEBA4 %_14.7 mM_ AgBF_4 _3 min and PEBA4 %_14.7 mM_ AgNO_3 _30 min will be designated in the text as PEBA_AgNP(AgBF_4) and PEBA_AgNP(AgNO_3), respectively.

The registered XRDP of these films are shown in Fig. 7. For comparison purposes, it included the XRDP of pure PEBA film. The amorphous structure of the copolymer is evidenced by the halo observed between 15° and 35° (Peyravi et al. 2010). No peaks corresponding to the crystalline AgNP were observed in the XRDP of the sample PEBA_AgNP(AgNO_3). This fact can be explained by the low amount of metallic silver present in this film (about 2.5 %, considering the concentration of 1 mM of AgNP). The PEBA_AgNP(AgBF_4) film shows peaks at 38° and 46° indexed to the planes (111) and (200) of the face-centered cubic lattice of silver. It is possible to observe that the presence of AgNP changes the structural arrangement of the polymer matrix, since the halo

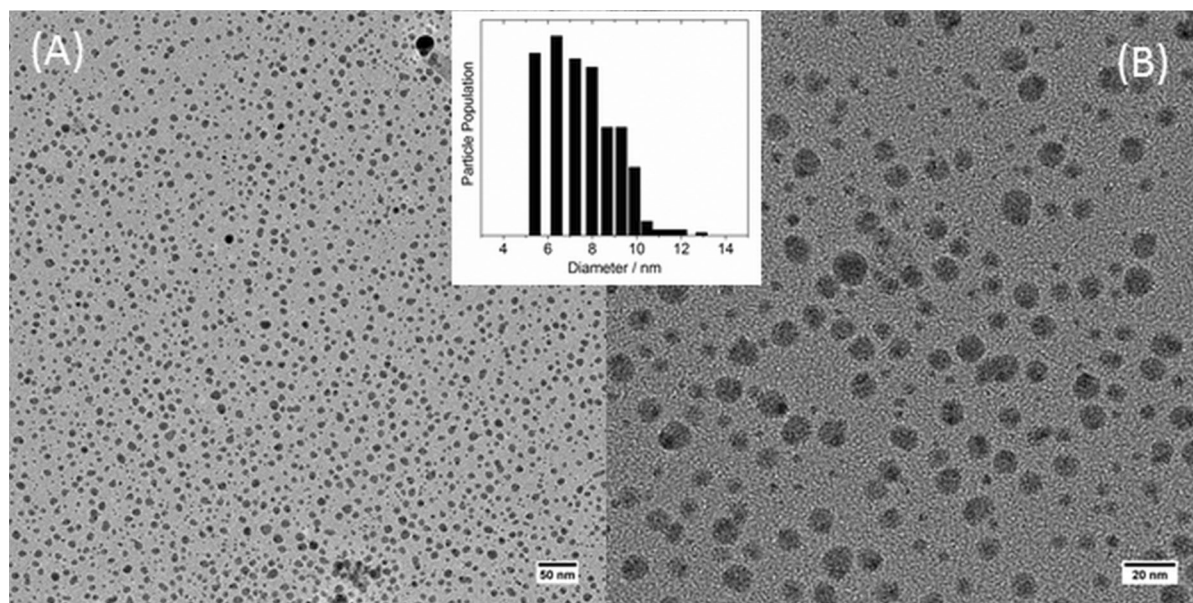


Fig. 6 TEM images of the PEBA4 %_{14.7} mM_{AgBF₄} 3 min dispersion in different magnifications. The *inset* shows the histogram of the particle size distribution

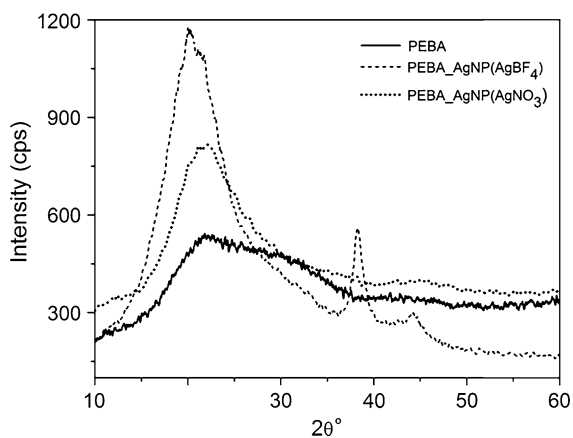


Fig. 7 XRD patterns of PEBA, PEBA_{AgNP(AgNO₃)}, and PEBA_{AgNP(AgBF₄)} films

became less broad and more intense in the samples containing silver.

The difference in the concentration of AgNP in the films is easily observed in the TGA analyses (Fig. 8). The residues of the sample PEBA_{AgNP(AgNO₃)} and PEBA_{AgNP(AgBF₄)} are around 2 and 10 %, respectively, which is coherent with the AgNP concentrations previously determined for the PEBA4 %_{14.7} mM_{AgBF₄} 3 min and PEBA4 %_{14.7} mM_{AgNO₃} 30 min dispersions. In the TGA curve of the

sample PEBA_{AgNP(AgNO₃)}, it is observed that the T_{onset} of the decomposition process occurs at the same temperature of the pure PEBA film (around 390 °C), indicating that the presence of AgNP did not reduce the thermal stability of the polymer. The same behavior was not observed in the TGA curve of the PEBA_{AgNP(AgBF₄)} film, where the high concentration of AgNP reduced the decomposition temperature of the polymer in 140 °C.

The registered vibrational spectra of pure PEBA and PEBA_{AgNP(AgNO₃)} and PEBA_{AgNP(AgBF₄)} films shown in Fig. 5S (supplementary material) indicate that the main chemical structure of the polymer is preserved. The main vibrational bands of pure PEBA, such as C=O (ester and amide) stretching at 1,730 and 1,640 cm^{-1} , N–H stretching at 3,300 cm^{-1} , C–O stretching at 1,100 cm^{-1} and the bands related to the vibrations of the carbon chain (axial and angular deformation) in 2,850, 2,920, 1,460, and 1,360 cm^{-1} are still present in the films containing AgNP.

Microbiological assays

Analyzing the circular “halo” or zone of inhibition that appears around the disk with high bacterial

concentration (10^8 CFU mL⁻¹) (Fig. 9), we can affirm that both bacteria, *Escherichia coli* (*E. coli*) and *Staphylococcus aureus* (*S. aureus*), are highly sensitive to the disks coated with the samples produced with 14.7 mM of AgNO₃ and 4 % (sample a), 3 % (sample

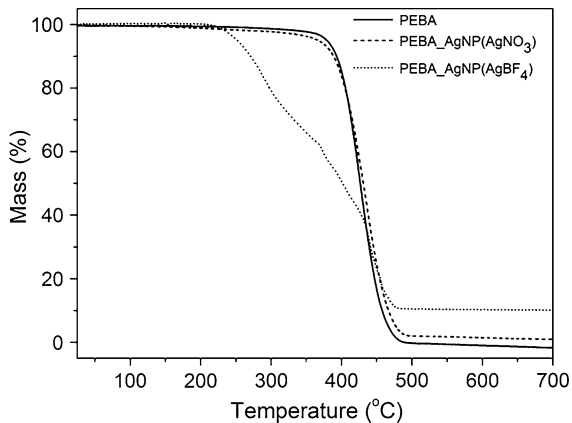


Fig. 8 TGA curves of PEBA, PEBA_AgNP(AgNO₃), and PEBA_AgNP(AgBF₄) films

b) or 2 % (sample c) of the PEBA refluxed during 30 min. The samples were diluted from 2.5 until 66 times in order to check if they lose effectiveness when diluted. Taking into account the sample a (concentration around 1 mM), it is possible to observe that even the most diluted sample (concentration around 0.015 mM) showed zone of inhibition for both bacteria when compared to the control.

When comparing the data of the samples a, b, and c for both bacteria, it can be seen that the samples a and b, with higher PEBA concentrations (3 and 4 %), show higher sensitivity than the sample c, containing just 2 % of PEBA. These data suggest that the aggregation of the AgNP in the sample containing 2 % of PEBA as referred in Fig. 3 may have been the explanation for the lowest antimicrobial activity. Even so, its antibacterial activity was in significant proportions.

Considering that the bacteria used were Gram-negative and Gram-positive, the antimicrobial action of all samples containing AgNP seems to act independently of their membrane molecular characteristics related to the bacteria. Interestingly, the samples seem

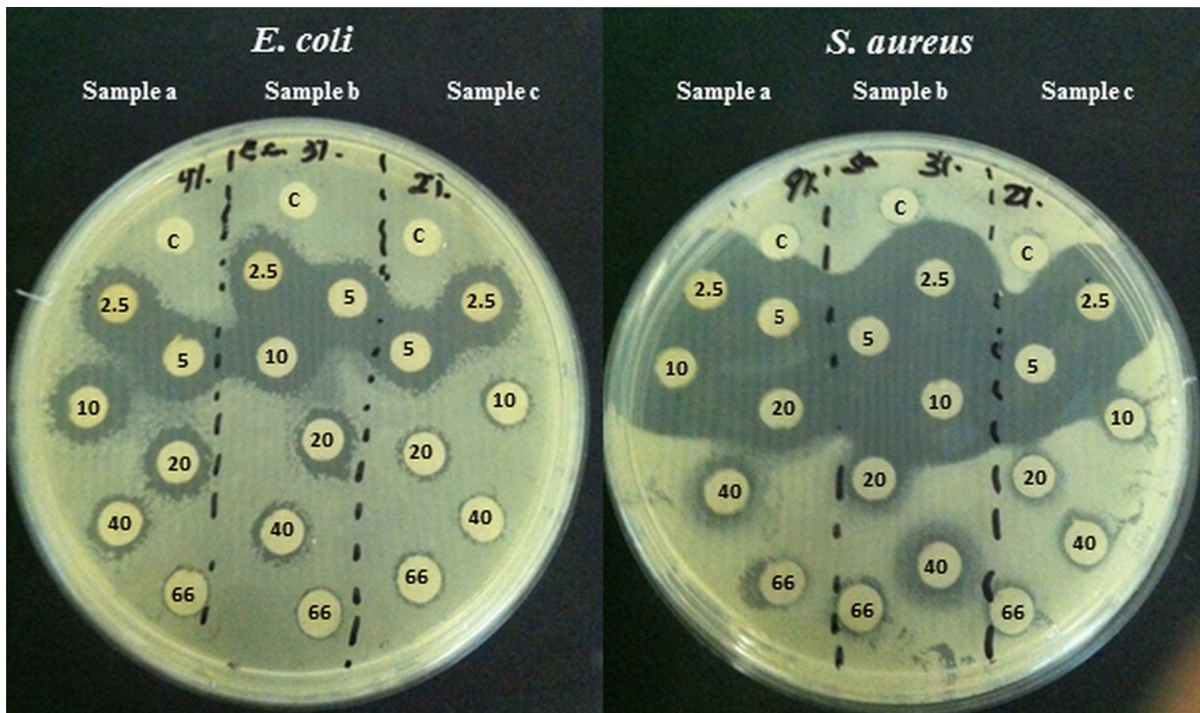


Fig. 9 Visual aspect of cultures obtained after 24 h of incubation. The disks were covered with AgNP dispersions produced by the use of 14.7 mM AgNO₃ solution and 4 % (sample a), 3 % (sample b) or 4 % (sample c) of PEBA refluxed

during 30 min. The disks marked with c are the controls (only PEBA solution). The numbers 2.5, 5, 10, 20, 40, and 66 represent the dilution factor of the AgNP stock solution

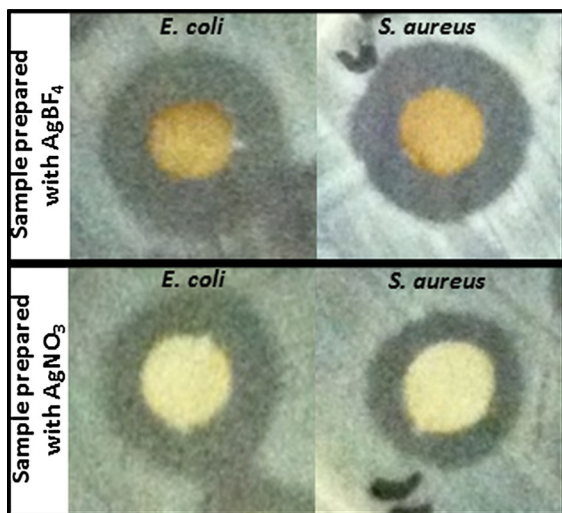


Fig. 10 Visual aspect of the bacterial sensitivity in cultures after 24 h of incubation of disks covered with the AgNP dispersions prepared with AgNO_3 and AgBF_4

to have a more effective action on Gram-positive bacteria (*Staphylococcus aureus*) based on the size of the halos and their sensitivity even at lower concentrations when compared with *E. coli* (Gram-negative). Further studies are needed to better elucidate this interesting phenomena.

Taking into account that the samples PEBA4 %_14.7mM_AgBF₄_3 min and PEBA4 %_14.7mM_AgNO₃_30 min are the most concentrated ones, they were analyzed comparatively in the microbiological assays. In Fig. 10, it can be observed that the AgNP dispersion prepared with AgBF_4 resulted in a larger halo than the one produced with the AgNO_3 for both bacteria. This fact can be explained by the difference of the AgNP concentration.

Conclusions

Hydrophobic AgNP dispersions obtained by reduction of silver cation by 1-butanol from two distinct sources (AgNO_3 and AgBF_4) in the presence of a biocompatible copolymer were produced in this work. The results showed that the dimension and concentration of silver nanoparticles are dependent on the copolymer and silver salt concentrations. Considering the best experimental conditions achieved, it produced dispersions composed of spherical silver nanoparticles with a diameter varying from 5 to 10 nm, with silver

concentration of 5 mM and long-term stability (more than a year). All dispersion showed very high antimicrobial activity against *E. coli* and *S. aureus* even when used at low concentration. These findings suggest the potential application of these dispersions as protective coatings for medical devices to prevent infections. However, this purpose still requires further studies to check the strength and the duration of the adhesiveness and the cytotoxicity of the films to human cells.

Acknowledgments The authors are thankful to Prof. Vera R. L. Constantino (IQ-USP) for the X-ray diffractometry experiments and to CESQ-POLI-USP for the TGA analysis. M.A. Bizeto is thankful to electron microscopy support of LNNano–Center for Nanoscience and Nanotechnology/MCT (research proposal TEM-MS 15017). F. F. Camilo is also thankful to CNPq for the financial support of this research (483878/2011-1).

References

- Alonso JC, Diamant R, Castillo P, Acosta-García MC, Batina N, Haro-Poniatowski E (2009) Thin films of nanoparticles deposited in vacuum by pulsed laser ablation using a YAG: Nd Laser. *Appl Surf Sci* 255:4933–4937
- Chen X, Schluesener HJ (2008) Nanosilver: a nanoproduct in medical application. *Toxicol Lett* 176:1–12
- Chen M, Feng Y-G, Wang X, Li T-C, Zhang J-Y, Qian D-J (2007) Silver nanoparticles capped by oleylamine: formation, growth, and self-organization. *Langmuir* 23:5296–5304
- Cumberland SA, Lead JR (2009) Particle size distributions of silver nanoparticles at environmentally relevant conditions. *J Chromatogr A* 1216:9099–9105
- Djebbar MK, Mguyen QT, Clement R, Germain Y (1998) Per-vaporation of aqueous ester solutions through hydrophobic poly(ether-block-amide) copolymer membranes. *J Membr Sci* 22:125–133
- Ferrando R, Jellinek J, Johnston RL (2008) Nanoalloys: from theory to applications of alloy clusters and nanoparticles. *Chem Rev* 108:845–910
- Ghosh KK, Kolay S (2008) Preparation of Ag nanoparticles in surfactant solution. *J Disp Sci Technol* 29:676–681
- Habibi B, Dadashpour E (2013) Electrooxidation of 2-propanol and 2-butanol on the Pt–Ni alloy nanoparticles in acidic media. *Electrochim Acta* 88:157–164
- Hu MZ, Easterly CE (2009) A novel thermal electrochemical synthesis method for production of stable colloids of “naked” metal (Ag) nanocrystals. *Mater Sci Eng C* 29:726–736
- Hunter E, Fendler JH (2004) Exploitation of localized surface Plasmon resonance. *Adv Mater* 16:1685–1706
- Jain PK, Huang X, El-Sayed IH, El-Sayed MA (2008) Nobel metals on the nanoscale: optical and photothermal properties and some applications in imaging, sensing, biology and medicine. *Acc Chem Res* 41:1578–1586

- Khanna PK, Singh N, Charan S, Subbarao VVS, Gokhale R, Mulik UP (2005) Synthesis and characterization of Ag/PVA nanocomposite by chemical reduction method. *Mater Chem Phys* 93:117–121
- Khaydarov RA, Khaydarov RR, Gapurova O, Estrin Y, Schepert T (2008) Electrochemical method for the synthesis of silver nanoparticles. *J Nanopart Res* 11:1193–1200
- Kim JS (2007) Reduction of silver nitrate in ethanol by poly(N-vinylpyrrolidone). *J Ind Eng Chem* 13:566–570
- Kontukhova EV, Buzin AI, Godovsky YK (2002) Melting of polyether block amide (Pebax): the effect of stretching. *Thermochim Acta* 391:271–277
- Krutyakov YA, Kudrinskiy AA, Olenin AY, Lisichkin GV (2008) Synthesis and properties of silver nanoparticles: advances and prospects. *Russ Chem Rev* 77:233–257
- Lee PC, Meisel D (1982) Adsorption and surface-enhanced Raman of dyes on silver and gold sols. *J Phys Chem* 86:3391–3395
- Lee GJ, Shin SI, Oh SG (2004) Preparation of silver dendritic nanoparticle using sodium polyacrylate in aqueous solution. *Chem Lett* 33:118–119
- Lide DR (2004) CRC handbook of chemistry and physics, 85th edn. CRC Press, Boca Raton
- Maillard M, Giorgio S, Pileni MP (2003) Tuning the size of silver nanodisks with similar aspect ratios: synthesis and optical properties. *J Phys Chem B* 107:2466–2470
- Nickel U, Castell AZ, Pöppl K, Schneider S (2000) A silver colloid produced by reduction with hydrazine as support for highly sensitive surface-enhanced Raman spectroscopy. *Langmuir* 16:9087–9091
- Patakfalvi R, Virányi Z, Dékány I (2004) Kinetics of silver nanoparticle growth in aqueous polymer solutions. *Colloid Polym Sci* 283:200–305
- Patakfalvi R, Diaz D, Velasco-Arias D, Rodriguez-Gattorno G, Santiago-Jacinto P (2008) Synthesis and direct interactions of silver colloidal nanoparticles with pollutant gases. *Colloid Polym Sci* 286:67–77
- Peyravi M, Babaluo AA, Ardestani MA, Aghjeh MKR, Pishghadam SR, Hadi P (2010) Study on the synthesis of poly(ether-block-amide) copolymer based on Nylon-6 and poly(ethylene oxide) with various block lengths. *J Appl Polym Sci* 118:1211–1218
- Pillai ZS, Kamat PV (2004) What factors control the size and shape of silver nanoparticles in the citrate ion reduction method? *J Phys Chem* 108:945–951
- Poole CP Jr, Owens FJ (2003) Introduction to nanotechnology. Wiley, New York
- Pradeep AT (2009) Noble metal nanoparticles for water purification: a critical review. *Thin Solid Films* 517:6441–6478
- Rao CNR, Müller A, Cheetham AK (2005) The chemistry of nanomaterials: synthesis, properties and applications. Wiley-VCH Verlag GmbH & Co, KGaA, Weinheim
- Ray PC (2010) Size and shape dependent second order nonlinear optical properties of nanomaterials and their application in biological and chemical sensing. *Chem Rev* 110:5332–5365
- Rodriguez-Gattorno G, Díaz D, Rendón L, Hernández-Segura GO (2002) Metallic nanoparticles from spontaneous reduction of silver (I) in DMSO. Interaction between nitric oxide and silver nanoparticles. *J Phys Chem B* 106:2482–2487
- Roduner E (2006) Size matters: why nanomaterials are different. *Chem Soc Rev* 35:583–592
- Rotello VM (2004) Nanoparticles building blocks for nanotechnology. Springer, New York
- Sharma VK, Yngard RA, Lin Y (2009) Silver nanoparticles: green syntheses and their antimicrobial activities. *Adv Colloid Interfac* 145:83–96
- Sileikaite A, Poisu J, Prosycevas I, Tamulevicius S (2009) Investigation of silver nanoparticles formation kinetics during reduction of silver nitrate with sodium citrate. *Mater Sci* 15:21–27
- Solomon SD, Bahadory M, Jeyarajasingam AV, Rutkowsky SA, Boritz C (2007) Synthesis and study of silver nanoparticles. *J Chem Educ* 84:322–325
- Sondi I, Salopek-Sondi B (2004) Silver nanoparticles as antimicrobial agent: a case study on *E. Coli* as a model for Gram-negative bacteria. *Adv Colloid Interfac* 275:177–182
- Sondi I, Goia DV, Matijević E (2003) Preparation of highly concentrated stable dispersions of uniform silver nanoparticles. *J Colloid Interf Sci* 260:75–81
- Suber L, Plunkett WR (2010) Formation mechanism of silver nanoparticle 1D microstructures and their hierarchical assembly into 3D superstructures. *Nanoscale* 2:128–133
- Suber L, Sondi I, Matijević E, Goia DV (2005) Preparation and the mechanisms of formation of silver particles of different morphologies in homogeneous solutions. *J Colloid Interf Sci* 288:489–495
- Sun Y, Yin Y, Mayers BT, Herricks T, Xia Y (2002) Uniform silver nanowires synthesis by reducing AgNO₃ with ethylene glycol in the presence of seeds and poly(vinylpyrrolidone). *Chem Mater* 12:4736–4745
- Tan Y, Li Y, Zhu D (2003) Preparation of silver nanocrystals in the presence of aniline. *J Colloid Interf Sci* 258:244–251
- Tolaymat TM, El Badawy AM, Genaidy A, Scheckel KG, Luxton TP, Suidan M (2010) An evidence-based environmental perspective of manufactured silver nanoparticle in syntheses and applications: a systematic review and critical appraisal of peer-reviewed scientific papers. *Sci Total Environ* 408:999–1006
- Wang H, Qiao X, Chena J, Wang X, Ding S (2005) Mechanisms of PVP in the preparation of silver nanoparticles. *Mater Chem Phys* 94:449–453
- Wang D, An J, Luo Q, Li X, Li M (2008) A convenient approach to synthesize stable silver nanoparticles and silver/poly-styrene nanocomposite particles. *J Appl Polym Sci* 110:3038–3046
- Yakovlev AV, Golubeva OY (2013) Optimization of the synthesis and study of stable aqueous dispersions of silver nanoparticles used in medicine. *Glass Phys Chem* 39:643–648
- Yang L, Li GH, Zhang JG, Zhang LD, Liu YL, Wang QM (2001) Fine structure of the plasmon resonance absorption peak of Ag nanoparticles embedded in partially oxidized Si matrix. *Appl Phys Lett* 78:102–104
- Yang J, Qi L, Lu C, Ma J, Cheng H (2005) Morphosynthesis of rhombododecahedral silver cages by self-assembly coupled with precursor crystal templating. *Angew Chem* 44:598–603
- Zielińska A, Skwarek E, Zaleska A, Gazda M, Hupka J (2009) Preparation of silver nanoparticles with controlled particle size. *Procedia Chem* 1:1560–1566